Chemical shift assignments for the *apo*-form of the catalytic domain, the linker region, and the carbohydrate-binding domain of the cellulose-active lytic polysaccharide monooxygenase *Sc*LPMO10C

Gaston Courtade[1], Zarah Forsberg[2], Gustav Vaaje-Kolstad[2], Vincent G. H. Eijsink[2], Finn L. Aachmann[1]

[1] NOBIPOL, Department of Biotechnology and Food Science, NTNU Norwegian University of Science and Technology, Sem Sælands vei 6/8, N-7491 Trondheim, Norway

2 Faculty of Chemistry, Biotechnology and Food Science, Norwegian University of Life Sciences, N-1432 Ås, Norway

To whom correspondence may be addressed: Finn L. Aachmann, E-mail: finn.l.aachmann@ntnu.no

Abstract

The *apo*-form of the 21.4 kDa catalytic domain and the 10.7 kDa carbohydrate binding domain of the AA10 family lytic polysaccharide monooxygenase *Sc*LPMO10C from *Streptomyces coelicolor* have been isotopically labeled and recombinantly expressed in *Escherichia coli*. In this paper, we report the ^{1}H, ^{13}C, and ^{15}N chemical shift assignments of each individual domain as well as an ensemble of the assignment for the full-length protein, including its approximately 30-amino acid long linker.

Keywords

Lytic polysaccharide monooxygenase, LPMO, AA10, cellulose, linker, CBM2

Biological context

Lytic polysaccharide monooxygenases (LPMOs) are copper-dependent enzymes that bind to the crystalline surface of polysaccharides (e.g. chitin and cellulose) and cause cleavage of β-1,4 glycosidic bonds by an oxidative mechanism. LPMO activity results in enhanced accessibility of the polysaccharides for their degradation by glycoside hydrolases. LPMOs comprise four of the auxiliary activity (AA) families of carbohydrate-active enzymes (AA9, AA10, AA11 and AA13) (Levasseur et al. 2013; Hemsworth et al. 2014; Lo Leggio et al. 2015; Beeson et al. 2015) that are active on several substrates. The unique role LPMOs play in efficient saccharification of lignocellulose gives them of great industrial and scientific interest (Johansen 2016).

*Sc*LPMO10C (previously known as CelS2) is a cellulose-active LPMO from *Streptomyces coelicolor* that produces C1-oxidized chain ends (i.e. aldonic acids) (Forsberg et al. 2011). *Sc*LPMO10C is composed of an N-terminal AA10 catalytic domain (hereafter called *Sc*AA10) connected by a linker of approximately 30-amino acids length to a C-terminal family 2 carbohydrate-binding module (hereafter called *Sc*CBM2). The structure of the *Sc*AA10 domain has been determined by X-ray crystallography, which depicts the typical LPMO β-sandwich fold decorated with loops and hydrophobic core densely packed with aromatic amino acids (Forsberg et al. 2014). The copper ion, which is an essential cofactor of all LPMOs, is located in the active site, coordinated in a histidine brace by the side-chain ($N^{\delta 1}$) and the □-amino nitrogen of the N-terminal histidine (His35) and the side-chain ($N^{\varepsilon 2}$) of His144. The active site is further shaped by Phe219, Ala142, Glu217 and Arg212. This copper coordination site is located in the center of a flat surface, which constitutes the putative substrate-binding site (Forsberg et al. 2014).

CBM2s represents a family of non-catalytic substrate-binding domains containing approximately 100 amino acids predominantly found in bacterial carbohydrate active enzymes. These domains principally have a cellulose-binding function (Jervis et al. 1997), but have also been demonstrated to bind xylan (Xu et al. 1995) and chitin (Nakamura et al. 2008). CBM2s are known to adopt a small β-sandwich fold, with the substrate binding site found on the face of one of the β-sheets (Boraston et al. 2004). The CBM2 in *Sc*LPMO10C has been shown to be

essential for binding to cellulose (REF Forsberg 2014b) and for higher yields of oxidized products (REF Forsberg 2014a).

Whereas catalytic domains of LPMOs have been in the spotlight since their discovery in 2010 (Vaaje-Kolstad et al. 2010), the role of CBMs in LPMO function is poorly understood. The few studies that have investigated their contribution to LPMO activity have reported lower product yields for truncated LPMOs compared to the full-length proteins (Crouch et al. 2016; Forsberg et al. 2016), probably caused by a reduced interaction with the substrate or by enzyme inactivation by destructive oxidative side reactions created by unbound LPMOs (Vaaje-Kolstad et al. 2017). NMR spectroscopy provides an opportunity to probe the structure of *Sc*CBM2, as well as the behavior of full-length *Sc*LPMO10C in solution, including its linker. The NMR assignment data presented here provides the first structural insights on a multi-modular LPMO, and it will allow future studies on the LPMO domain, the CBM2 domain, the linker region, and the interaction between the domains.

Methods and experiments

The NMR assignment was performed separately on the *apo*-form of the recombinantly expressed catalytic domain of *Sc*LPMO10C (*Sc*AA10) and its CBM2 (*Sc*CBM2), prior to assembling each of the assignments on the full-length protein.

Cloning, production and purification of *Sc*AA10 was performed as described previously, using the LPMO expression cassette (Courtade et al. 2017). In summary, the catalytic domain of *Sc*LPMO10C (Uniprot ID: Q9RJY2; residues 35-230) was cloned downstream of the signal sequence of *Sm*LPMO10A from *Serratia marcescens*, resulting in the vector pJB_SP_*Sc.* Recombinant *E. coli* RV308 (pJB_SP_*Sc*) were grown in M9 medium containing ^{13}C and ^{15}N- or ^{15}N-isotopes (6 g/L Na_2HPO_4, 3 g/L KH_2PO_4, 0.5 g/L NaCl) supplemented with 98% $(^{15}NH_4)_2SO_4$, 4 g/L ^{13}C- or natural abundance glucose, 10 mL Bioexpress Cell Growth Media (Cambridge Isotope Laboratories, Tewksbury, MA, USA), 5 mL Gibco™ MEM Vitamin Solution (100x) (Thermo Fisher Scientific), 2 mM $MgSO_4$, 10 mL Trace Metal solution and ampicillin (100 µg/mL). Pre-cultures of 10 mL LB were inoculated with recombinant cells and grown at 30 °C and 225 rpm overnight. Main cultures of 500 mL M9 medium were made in shaking flasks, inoculated with 1% pre-culture and incubated at 30 °C and 225 rpm to $OD_{600\ nm}$ ~0.8. The culture was cooled on ice for 5 min, induced with 0.1 mM *m*-toluic acid and further incubated at 16 °C and 225 rpm for 20 h. Pelleted cells were subjected to an osmotic shock treatment and the periplasmic extract was purified by ion exchange using a 5 mL HiTrap® DEAE FF anion exchanger (GE Life Sciences), and by size-exclusion chromatography using a HiLoad® 16/600 Superdex® 75 pg column (GE Life Sciences) as previously described (REF Forsberg 2014a).

Cloning of *Sc*CBM2 was performed by ligation-independent cloning as previously described (Aslanidis and de Jong 1990), essentially cloning the *Sc*CBM2 coding region (residues 261-364) from pRSETB_*cels2* opt (Forsberg et al. 2014) to the pNIC-CH expression vector (AddGene), with a C-terminal His-tag.

Cloning of full-length *Sc*LPMO10C was performed by sequence- and ligation-independent cloning as described by Jeong et al. (Jeong et al. 2012). The *Sc*LPMO10C coding region (residues 35-364) was cloned into the Expresso™ pETite N-His SUMO T7 expression vector (Lucigen), ensuring that the N-terminal histidine of *Sc*LPMO10C was placed immediately after the SUMO protease cleavage site.

Production and purification of *Sc*CBM2 and SUMO-fused *Sc*LPMO10C was performed as follows.

Pre-cultures were made by inoculating 5 mL LB supplemented with kanamycin (50 µg/mL) with recombinant *E. coli* T7 express (pNIC_*Sc*CBM2) or HI-Control™ BL21(DE3) (pETite_SUMO_ *Sc*LPMO10C) and incubating at 30 °C and 225 rpm for 7 h. Main cultures of 500 mL ^{13}C and ^{15}N- or ^{15}N-isotope containing M9 medium supplemented with kanamycin (50 µg/mL) were made in shaking flasks by inoculating with 0.8% pre-culture and incubating at 22 °C and 225 rpm for 18 h to $OD_{600\ nm}$ ~0.8. The culture was induced with 0.5 mM IPTG followed by incubation at 22 °C and 225 rpm for 24 h. Cells were harvested by centrifugation for 10 min at 5000 x g and 4 °C and the pellet was stored at -18 °C prior to purification. The pellet was resuspended in 19 mL lysis buffer (50 mM Na-phosphate pH 8.0, 50 mM NaCl, 0.05% Triton™ X-100) with half-a-tablet EDTA-free cOmplete™ ULTRA protease inhibitor (Roche) and sonicated using a Branson Sonifier equipped with a microtip. The suspension was centrifuged for 25 min at 23,000 x g and 4 °C and sterilized by filtration (0.2 µm). An Econo-Column® (Bio-Rad) containing 2 mL Ni-NTA Agarose (QIAGEN) was equilibrated with 40 mL wash and elution

buffer (WEB; 50 mM Trizma® HCl pH 8.0, 300 mM NaCl) with 20 mM imidazole. 1 mL WEB buffer with 400 mM imidazole was added to the filtrate, and loaded on the column. After 20 min, the column was emptied and then fractionated using the following elution steps with increasing imidazole concentration: two fractions eluted with 10 mL WEB (20 mM imidazole) each, one fraction eluted with 10 mL WEB (40 mM imidazole), one fraction eluted with 10 mL WEB (100 mM imidazole), one fraction eluted with 5 mL WEB (200 mM imidazole) and 2 mL WEB (400 mM imidazole), and one fraction eluted with 10 mL WEB (400 mM imidazole). SUMO-fused *Sc*LPMO10C began to elute at 40 mM imidazole, while *Sc*CBM2 eluted at 100 mM imidazole.

Elution fractions that contained SUMO-fused *Sc*LPMO10C were pooled and concentrated to 2.5 mL using Vivaspin® 20 protein spin concentrators (10 kDa cut-off, Sartorius). The solution was diluted 10-fold with cleaving buffer (25 mM Trizma® HCl pH 8.0, 150 mM NaCl, 10% glycerol) dithiothreitol (DTT) was added to a final concentration of 2 mM, followed by 3-5 µL SUMO Express Protease (Lucigen). The solution was incubated at 4 °C overnight prior to repeating the His-tag purification as described above. Both the SUMO fusion tag and the SUMO Express Protease contain His-tags, but cleaved *Sc*LPMO10C does not. Therefore, pure *Sc*LPMO10C was obtained in the flow-through and in the fractions eluted with WEB containing 20 mM imidazole.

Fractions of *Sc*CBM2, *Sc*AA10 or full-length *Sc*LPMO10C were identified using SDS-PAGE and subsequently pooled, concentrated and the buffer exchanged to 25 mM sodium phosphate buffer pH 5.5 and 10 mM NaCl in 90% H_2O/10% D_2O, using a Vivaspin® 20 protein spin concentrators (10 kDa cut-off, Sartorius). The protein concentration was determined by measuring the A_{280} of the protein solution using a NanoDrop ND-1000 spectrophotometer (Thermo Fisher Scientific) and deducing the protein concentration based on the theoretical extinction coefficient (calculated using the ProtParam tool; http://web.expasy.org/tools/protparam/) (Gasteiger et al. 2005).

The NMR spectra were recorded at 25 °C on a Bruker Ascend 800 MHz spectrometer Avance III HD or a Bruker 600 MHz spectrometer Avance III, both equipped with a 5 mm Z-gradient CP-TCI (H/C/N) cryoprobe at the NV-NMR-Center/Norwegian NMR Platform in Trondheim, Norway. ^{1}H shifts were referenced internally to HDO, while ^{13}C and ^{15}N chemical shifts were referenced indirectly to HDO, based on the absolute frequency ratios (Zhang et al. 2003). Spectra used for the sequence-specific assignments of *Sc*CBM2 and *Sc*AA10, as well as for the assignment of the linker region in full-length *Sc*LPMO10C are listed in Table 1. The backbone assignment of full-length *Sc*LPMO10C was performed by assembling together the assignments of *Sc*CBM2 and *Sc*AA10 and repositioning the peaks that had shifted by using the spectra listed in Table 1.

Table 1. Spectra used for the assignments of *Sc*CBM2, *Sc*AA10 and the linker region of full-length *Sc*LPMO10C.

Protein	*Sc*CBM2	*Sc*AA10	Linker in full-length *Sc*LPMO10C
Extent of the assignment	Backbone and all side-chains	Backbone and aliphatic side-chains	Backbone
Spectra	^{15}N-HSQC, ^{13}C-aliphatic HSQC, ^{13}C-aromatic HSQC, HNHA, HNCO (NUS), HN(CA)CO (NUS), HNCA (NUS), HN(CO)CACB (NUS), aliphatic H(C)CH-TOCSY, CACO, CON, ^{15}N-edited NOESY-HSQC, and ^{13}C-edited aliphatic and aromatic NOESY-HSQC	^{15}N-HSQC, ^{13}C-aliphatic HSQC, HNCA, HN(CO)CA, HNCO, HN(CA)CO, CBCANH, CBCA(CO)NH, HBHA(CO)NH, aliphatic H(C)CH-TOCSY, and ^{13}C-edited aliphatic NOESY-HSQC	^{15}N-HSQC (TROSY), HNCO (TROSY), HN(CA)CO (TROSY), HNCA, CBCA(CO)NH (TROSY), CBCANH (TROSY)

The NMR data were recorded and processed with Bruker TopSpin version 3.2/3.5 and spectral analysis was performed using CARA version 1.5.5 (Keller 2004). Certain spectra were recorded with non-uniform sampling (NUS) and processed using compressed sensing (Kazimierczuk and Orekhov 2011) in MddNMR version 2.0 (Orekhov and Jaravine 2011). Secondary structure elements were analyzed using the web-based version of the TALOS-N software (http://spin.niddk.nih.gov/bax/software/TALOS-N/) (Shen and Bax 2013) using the ^{13}C/^{15}N chemical shifts. Secondary structure propensity was also analyzed using SSP (Secondary Structure Propensities from chemical shifts) (Marsh et al. 2006), using C^{α}, C^{β} and C'chemical shifts.

Assignment and data deposition

We report here the assignment of the backbone and side-chain resonances of *Sc*CBM2 (H^N, H^α, N, C^α, C' > 97%; Aliphatic and aromatic side-chains > 75%) and *Sc*AA10 (H^N, H^α, N, C^α, C' > 90%; Aliphatic side-chains > 80%). The ^{15}N-HSQC spectra, together with the assignment of the resonances is shown in Fig. 1 and 2. Exchangeable side-chain protons were not assigned, nor were the aromatic side-chains of *Sc*AA10. Moreover, we report the assignment of the backbone of full-length *Sc*LPMO10C. The backbone assignments for *Sc*CBM2 and *Sc*AA10 were used as a basis for the assignment of full-length *Sc*LPMO10C, but this assignment was accomplished on its own using the experiments shown in Table 1. A high degree of overlap between the signals of the linker region and the catalytic domain in full-length *Sc*LPMO10C impeded the assignment of the signals from the catalytic domain, resulting in an assignment completion for full-length *Sc*LPMO10C (H^N, N, C^α, C', C^β) of about 60%. Nevertheless, over 80% of the aforementioned chemical shifts in the linker region in full-length *Sc*LPMO10C were assigned. The ^{15}N-HSQC spectra, together with the assignment of the resonances is shown in Fig. 3. H^N, N chemical shifts from this spectrum can be overall superimposed with the chemical shifts in Fig. 1 and 2. The chemical shift data for all three assignments have been deposited in the Biological Magnetic Resonance Data Bank (BMRB) under the accession number 27078.

Secondary structure analysis

Analysis of the secondary structure elements of *Sc*AA10 both by itself and in full-length *Sc*LPMO10C indicated the presence of two α-helical segments and 7-8 β-strands (Fig. 4 panels A and B). The length and position of these secondary structure elements was in good agreement with those observed in the X-ray crystal diffraction structure of *Sc*AA10 (PDB ID: 4OY7) (Forsberg et al. 2014), with exception of helical structures present in the crystal structure that were not identified by TALOS-N. Moreover, secondary structure elements identified in *Sc*CBM2 both by itself and in the full-length protein indicate an overall β-strand propensity (Fig. 4, panels A and C), a common feature for family 2 CBMs (Boraston et al. 2004). Interestingly, the secondary structure propensity for the linker region in full-length *Sc*LPMO10C suggest a β-strand region, this is likely an indication that the linker is an elongated structure, which is expected for a Thr-Pro linker (George and Heringa 2002). Overall, it would seem that the secondary structure elements in each of the individual domains persists when they are joined together in full-length *Sc*LPMO10C.

Acknowledgements

This work was financed by SO-funds from NTNU Norwegian University of Science and Technology and by the MARPOL project, the Norwegian NMR Platform, both from the Research Council of Norway (grant numbers 221576, 226244, respectively).

Conflict of interest

The authors declare that they have no conflict of interest.

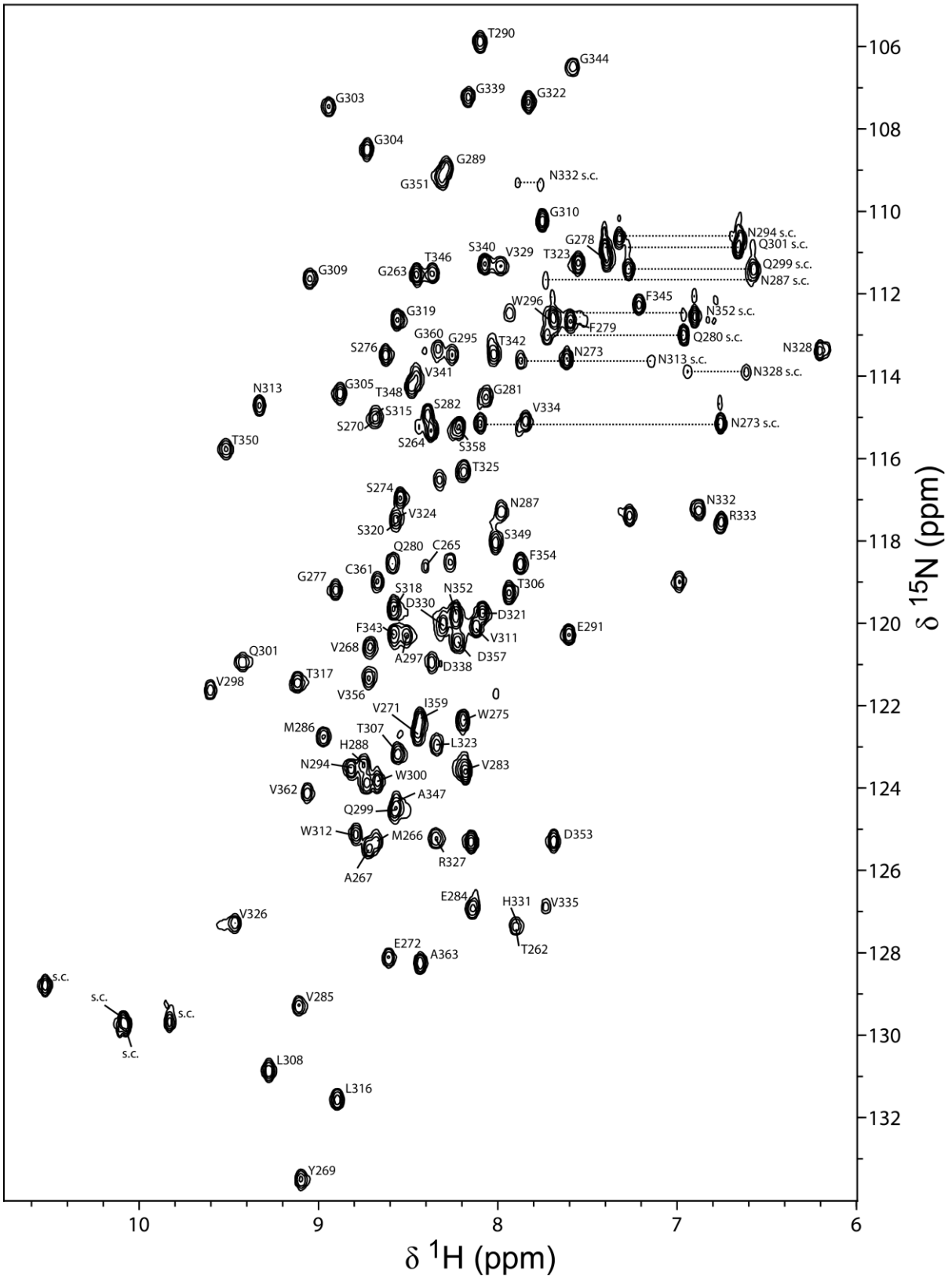

Fig. 1 ^{1}H, ^{15}N HSQC spectrum of ^{13}C, ^{15}N-labeled *Sc*CBM2 (0.5 mM) from *S. coelicolor* in (90:10) H_2O:D_2O in 20 mM Na-phosphate buffer pH 5.5 with 10 mM NaCl, at 298 K. Unassigned side-chains are labeled as "s.c.".

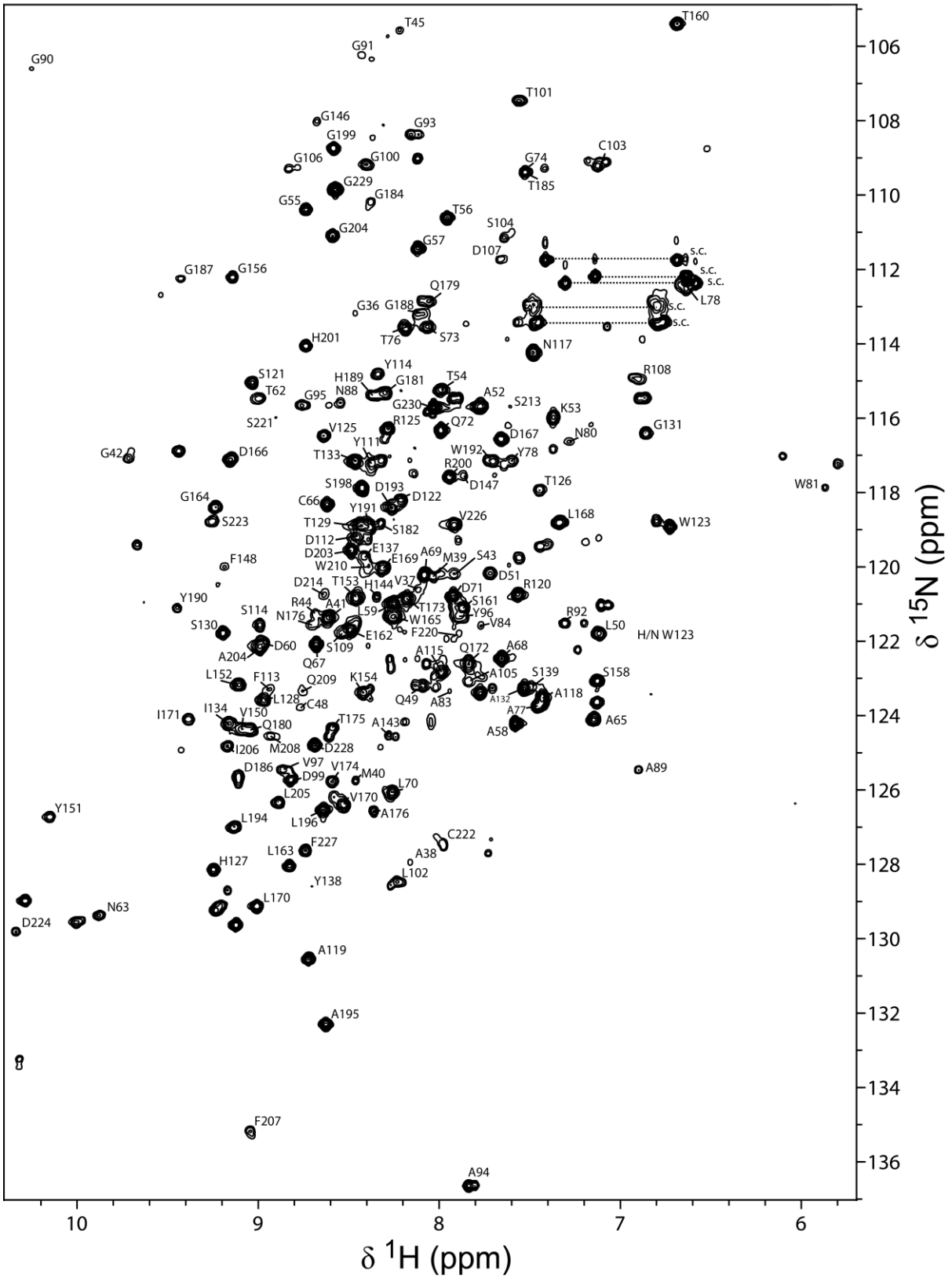

Fig. 2 ^{1}H, ^{15}N HSQC spectrum of ^{13}C, ^{15}N-labeled *apo*-form of the N-terminal catalytic domain (*Sc*AA10) from *Sc*LPMO10C (0.5 mM) in (90:10) H_2O:D_2O in 20 mM Na-phosphate buffer pH 5.5 with 10 mM NaCl, at 298 K. Unassigned side-chains are labeled as "s.c.".

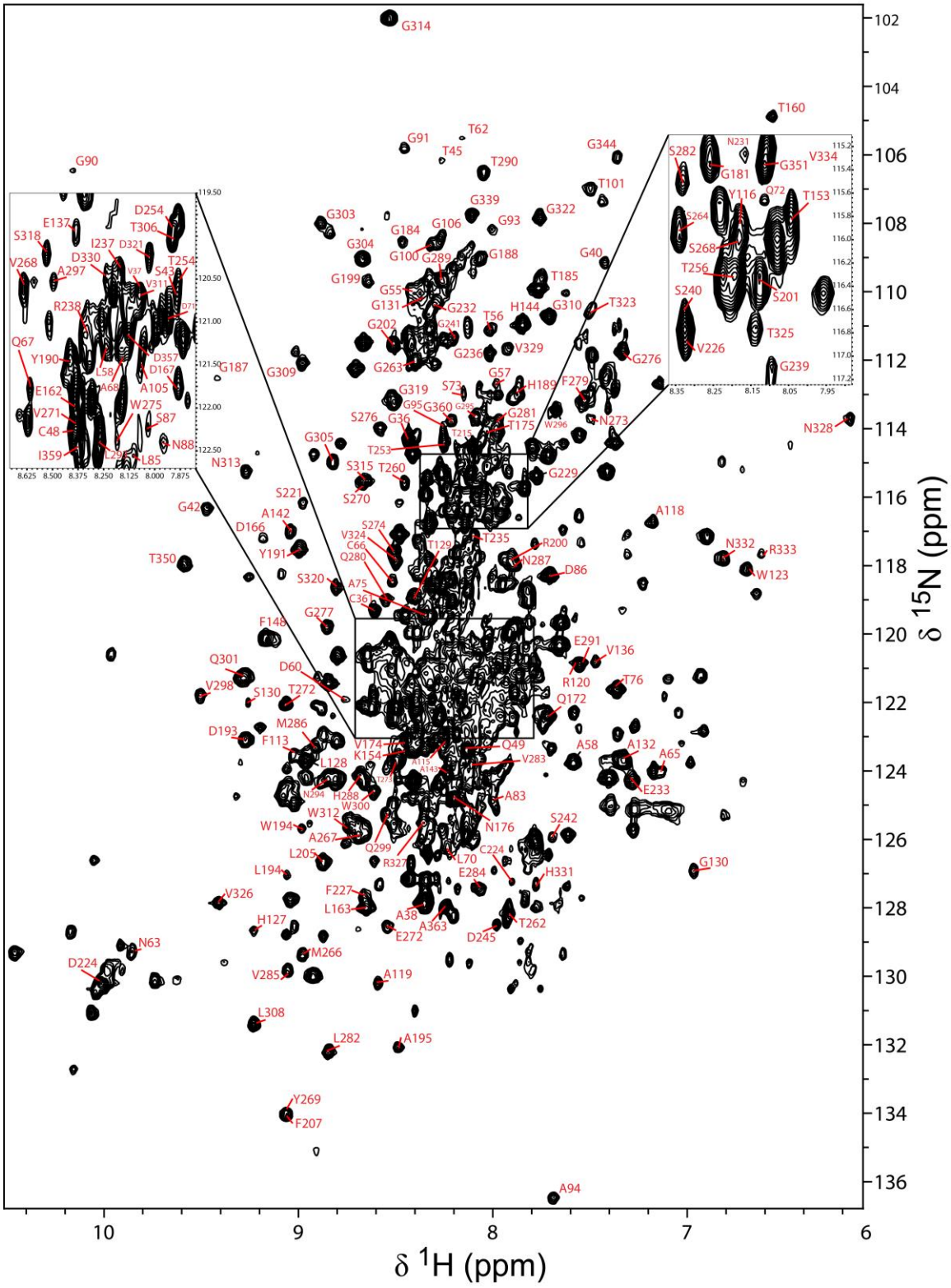

Fig. 3 ^{1}H, ^{15}N HSQC spectrum of ^{13}C, ^{15}N-labeled full-length *apo*-*Sc*LPMO10C (0.3 mM) from *S. coelicolor* in (90:10) H_2O:D_2O in 20 mM Na-phosphate buffer pH 5.5 with 10 mM NaCl, at 298 K. Residue types and numbers are indicated. Unassigned signals likely arise from the proteolytically cleaved SUMO-tag.

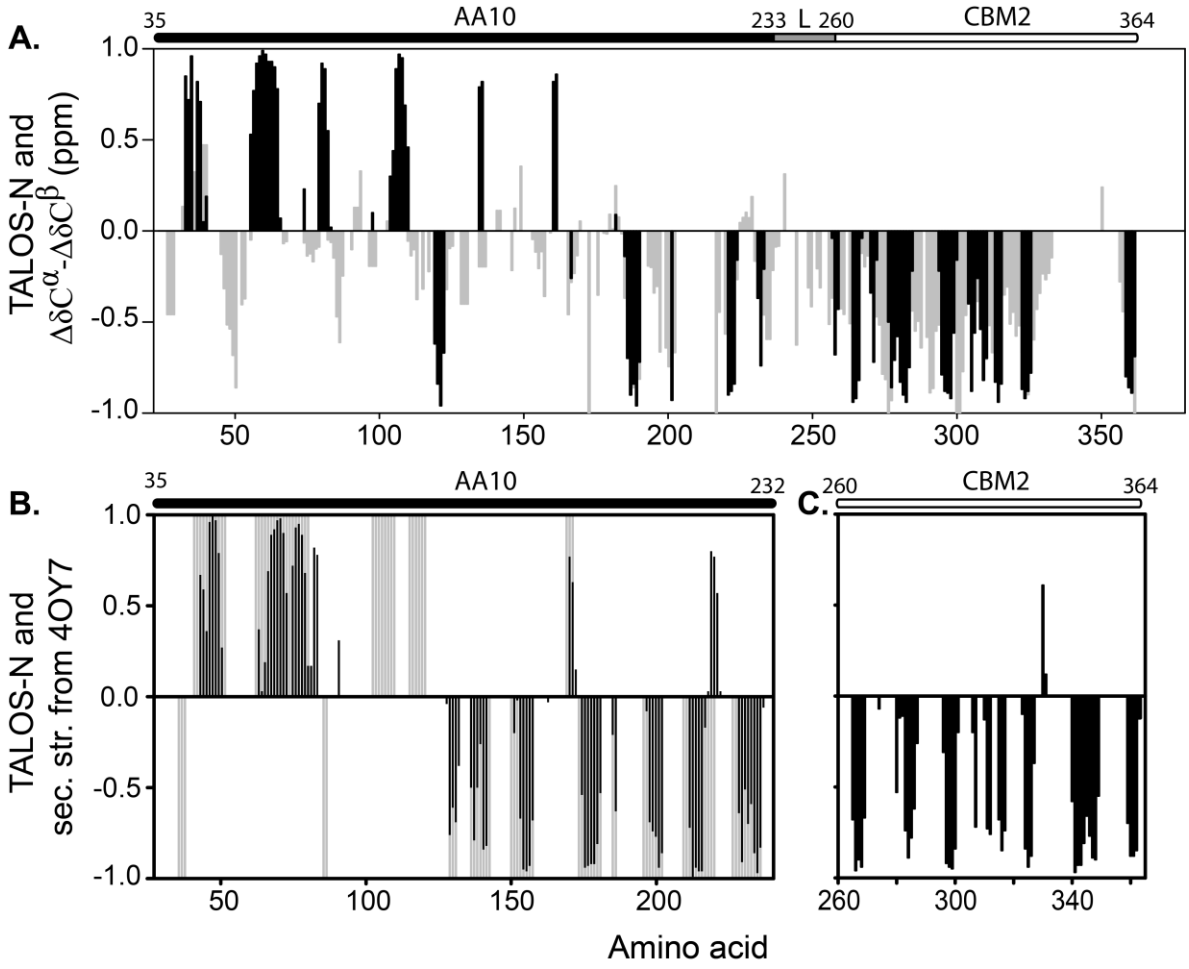

Fig. 4 (A) Secondary structure propensity for full-length *Sc*LPMO10C analyzed by TALOS-N (black) and $\Delta\delta C^{\alpha}$-$\Delta\delta C^{\beta}$ secondary chemical shifts (grey). (B) Secondary structure propensity for *Sc*AA10 analyzed by TALOS-N (black) together with secondary structure from the X-ray crystal diffraction structure of *Sc*AA10 (PDB ID: 4OY7; grey). (C) Secondary structure propensity for *Sc*CBM2 analyzed by TALOS-N (black). Positive values indicate α-helical propensity and negative values indicate β-strand propensity. In the linker region (labeled "L"), negative values indicate an elongated structure.

References

Aslanidis C, de Jong PJ (1990) Ligation-independent cloning of PCR products (LIC-PCR). Nucleic Acids Res 18:6069–6074. doi: 10.1093/nar/18.20.6069

Beeson WT, Vu V V, Span EA, et al (2015) Cellulose degradation by polysaccharide monooxygenases. Annu Rev Biochem 84:923–946. doi: 10.1146/annurev-biochem-060614-034439

Boraston AB, Bolam DN, Gilbert HJ, Davies GJ (2004) Carbohydrate-binding modules: fine-tuning polysaccharide recognition. Biochem J 382:769–781. doi: 10.1042/BJ20040892

Courtade G, Le SB, Sætrom GI, et al (2017) A novel expression system for lytic polysaccharide monooxygenases. Carbohydr Res. doi: 10.1016/j.carres.2017.02.003

Crouch LI, Labourel A, Walton PH, et al (2016) The contribution of non-catalytic carbohydrate binding modules to the activity lytic polysaccharide monooxygenases. J Biol Chem 291:7439–7449. doi: 10.1074/jbc.M115.702365

Forsberg Z, Mackenzie AK, Sørlie M, et al (2014) Structural and functional characterization of a conserved pair of bacterial cellulose-oxidizing lytic polysaccharide monooxygenases. Proc Natl Acad Sci U S A 111:8446–8451. doi: 10.1073/pnas.1402771111

Forsberg Z, Nelson CE, Dalhus B, et al (2016) Structural and functional analysis of a lytic polysaccharide monooxygenase important for efficient utilization of chitin in *Cellvibrio japonicus*. J Biol Chem 291:7300–7312. doi: 10.1074/jbc.M115.700161

Forsberg Z, Vaaje-Kolstad G, Westereng B, et al (2011) Cleavage of cellulose by a CBM33 protein. Protein Sci 20:1479–1483. doi: 10.1002/pro.689

Gasteiger E, Hoogland C, Gattiker A, et al (2005) Protein identification and analysis tools on the ExPASy server. In: Walker JM (ed) The Proteomics Protocols Handook. Springer, pp 571–607

George RA, Heringa J (2002) An analysis of protein domain linkers: their classification and role in protein folding. Protein Eng 15:871–879. doi: 10.1093/PROTEIN/15.11.871

Hemsworth GR, Henrissat B, Davies GJ, Walton PH (2014) Discovery and characterization of a new family of lytic polysaccharide monooxygenases. Nat Chem Biol 10:122–126. doi: 10.1038/nchembio.1417

Hemsworth GR, Johnston EM, Davies GJ, Walton PH (2015) Lytic polysaccharide monooxygenases in biomass conversion. Trends Biotechnol 33:747–761. doi: 10.1016/j.tibtech.2015.09.006

Jeong JY, Yim HS, Ryu JY, et al (2012) One-step sequence-and ligation-independent cloning as a rapid and versatile cloning method for functional genomics studies. Appl Environ Microbiol 78:5440–5443. doi: 10.1128/AEM.00844-12

Jervis EJ, Haynes CA, Kilburn G, et al (1997) Surface diffusion of cellulases and their isolated binding domains on cellulose surface. J Biol Chem 272:24016–24023. doi: 10.1074/jbc.272.38.24016

Johansen KS (2016) Lytic polysaccharide monooxygenases: the microbial power tool for lignocellulose degradation. Trends Plant Sci 21:926–936. doi: 10.1016/j.tplants.2016.07.012

Kazimierczuk K, Orekhov VY (2011) Accelerated NMR spectroscopy by using compressed sensing. Angew Chemie - Int Ed 50:5556–5559. doi: 10.1002/anie.201100370

Levasseur A, Drula E, Lombard V, et al (2013) Expansion of the enzymatic repertoire of the CAZy database to integrate auxiliary redox enzymes. Biotechnol Biofuels 6:41–54. doi: 10.1186/1754-6834-6-41

Lo Leggio L, Simmons TJ, Poulsen JN, et al (2015) Structure and boosting activity of a starch-degrading lytic polysaccharide monooxygenase. Nat Commun 6:1–9. doi: 10.1038/ncomms6961

Marsh J a, Singh VK, Jia Z, Forman-Kay JD (2006) Sensitivity of secondary structure propensities to sequence differences between alpha- and gamma-synuclein: implications for fibrillation. Protein Sci 15:2795–2804. doi: 10.1110/ps.062465306

Nakamura T, Mine S, Hagihara Y, et al (2008) Tertiary structure and carbohydrate recognition by the chitin-binding domain of a hyperthermophilic chitinase from *Pyrococcus furiosus*. J Mol Biol 381:670–680. doi:

10.1016/j.jmb.2008.06.006

Orekhov VY, Jaravine VA (2011) Analysis of non-uniformly sampled spectra with multi-dimensional decomposition. Prog Nucl Magn Reson Spectrosc 59:271–292. doi: 10.1016/j.pnmrs.2011.02.002

Shen Y, Bax A (2013) Protein backbone and sidechain torsion angles predicted from NMR chemical shifts using artificial neural networks. J Biomol NMR 56:227–41. doi: 10.1007/s10858-013-9741-y

Vaaje-Kolstad G, Forsberg Z, Loose JS, et al (2017) Structural diversity of lytic polysaccharide monooxygenases. Curr Opin Struct Biol 44:67–76. doi: 10.1016/j.sbi.2016.12.012

Vaaje-Kolstad G, Westereng B, Horn SJ, et al (2010) An oxidative enzyme boosting the enzymatic conversion of recalcitrant polysaccharides. Science 330:219–222. doi: 10.1126/science.1192231

Xu GY, Ong E, Gilkes NR, et al (1995) Solution structure of a cellulose-binding domain from *Cellulomonas fimi* by nuclear magnetic resonance spectroscopy. Biochemistry 34:6993–7009. doi: 10.1021/bi00021a011

Zhang H, Neal S, Wishart DS (2003) RefDB: a database of uniformly referenced protein chemical shifts. J Biomol NMR 25:173–95. doi: 10.1023/A:1022836027055